

SIMULATION AND EXPERIMENTAL INVESTIGATION OF HEAVY ION INDUCED DESORPTION FROM CRYOGENIC TARGETS*

Ch. Maurer[†], D.H.H. Hoffmann, Institut für Kernphysik, TU Darmstadt, Germany
 L.H.J. Bozyk, H. Kollmus, P.J. Spiller, GSI, Darmstadt, Germany

Abstract

Heavy-ion impact induced gas desorption is the key process that drives beam intensity limiting dynamic vacuum losses. Minimizing this effect, by providing low desorption yield surfaces, is an important issue for maintaining a stable ultra high vacuum during operation with medium charge state heavy ions. For room temperature targets, investigations show a scaling of the desorption yield with the beam's near-surface electronic energy loss, i.e. a decrease with increasing energy [1, 2]. An optimized material for a room temperature ion-catcher has been found. But for the planned superconducting heavy-ion synchrotron SIS100 at the FAIR accelerator complex, the ion catcher system has to work in a cryogenic environment. Desorption measurements with the prototype cryocatcher for SIS100 showed an unexpected energy scaling [3], which needs to be explained. Understanding this scaling might lead to a better suited choice of material, resulting in a lower desorption yield. Here, new experimental results will be presented along with insights gained from gas dynamics simulations.

MEASUREMENT OF CRYOGENIC DESORPTION

In this experiment, a cryogenic target is placed in a UHV environment and cooled by a coldhead. After the impact of a heavy ion beam, the resulting pressure evolution is measured. In combination with the beam intensity, a desorption yield η is calculated. It is defined as the number of desorbed gas particles divided by the number of impacting beam ions. A detailed description of the measurement setup can be found in [4].

While the beam's intensity can be measured with a beam current transformer, identifying the number of desorbed particles is more difficult. Up to now, the ideal gas law was employed to calculate this number by using the measured peak pressure after beam impact in a defined volume. A gas dynamics simulation can improve the analysis.

Another improvement compared to [4] is the extended range of experimental parameters, especially regarding the target. The target assembly is connected to a coldhead to facilitate a cryogenic environment and incorporates an optional thermal shield. Electrical insulation of the target is necessary to measure the ion current caused by the beam impact. It is achieved through a nonconducting tile, which unfortunately also limits the heat flow towards the coldhead. First results, obtained with a U^{73+} beam, an Al_2O_3 -ceramic

insulation plate, and a target made from gold coated copper have already been presented. Further experiments were conducted with a target made from uncoated stainless steel, but also without a thermal shield. In a later experiment, a Bi^{68+} -beam was used with the copper target and a thermal shield.

NEW EXPERIMENTAL RESULTS

Changing the target materials introduces several variations into the experiment. A modification in thermal conductivity leads to a shift of the thermal equilibrium between external heat load and heat transfer towards the coldhead. Thus, the lowest achievable temperature T_{min} rises when exchanging the copper target with a stainless steel target because copper has a higher thermal conductivity than steel.

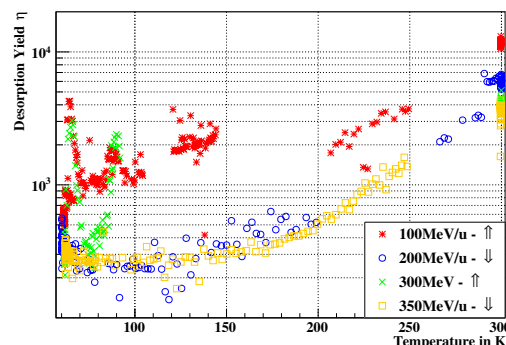


Figure 1: Temperature dependant desorption yield η for a U^{73+} -beam on a steel target.

The first modification was performed by exchanging the copper target with a stainless steel target. The results from this experiment are presented in Figs. 1 and 2.

The desorption yield decreases by an order of magnitude between room temperature and 100 K. The previously encountered desorption peak around 50 K can be found again when measuring with a deactivated coldhead on a rising temperature slope. After reaching room temperature, η again scales with $(dE/dx)^2$. Furthermore, a comparison of the absolute room temperature values with [1] and [3] shows a discrepancy by two orders of magnitude. The much higher η measured here might be a result of the milder bakeout process that had to be employed to protect the coldhead. Furthermore, the η measured with the copper target is twice as high as the η measured for the steel target at room temperature. This contradicts previous findings.

For cryogenic temperatures, the $(dE/dx)^2$ scaling can also be observed while the previously encountered, well

* This project is funded by the german ministry for education and research (FKZ 06DA7031)

[†] c.maurer@gsi.de

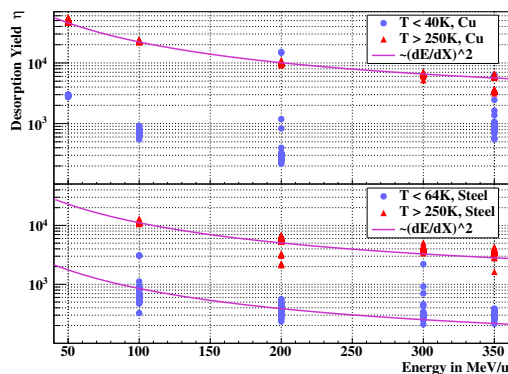


Figure 2: Comparison between the energy dependance of η at cryogenic and at room temperature for a U^{73+} -beam on a gold coated copper and an uncoated steel target. The lower panel has been compiled from the same dataset as Fig. 1. Both experiments were conducted without a thermal shield.

pronounced minimum at 200 MeV/u is no longer visible. Possible reasons for this discrepancy might be the significantly higher T_{min} , a peculiarity of the material or an erroneous measurement in the copper beamtime that underestimates η for the 200 MeV/u dataset or overestimates it for the 350 MeV/u dataset. However, the raw data on which these values are based has been rechecked and no anomalies have been found.

Another experiment was performed with a Bi^{68+} beam, the gold coated copper target, and a thermal shield. The result is presented in Fig. 3. The room temperature plot is very similar to the one presented in the lower panel of Fig. 2, but the cryogenic η behaves different. Here, no order of magnitude difference between the cryogenic and the room temperature measurements can be found. An explanation for this different behaviour is outstanding.

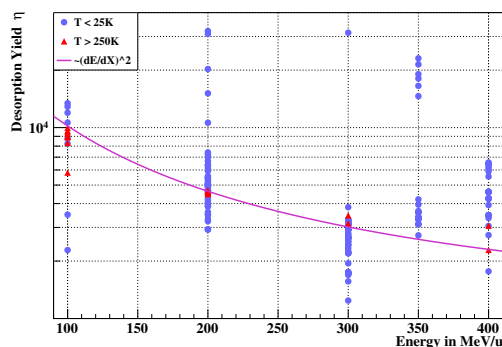


Figure 3: The energy dependance of η at cryogenic and at room temperature for a Bi^{68+} -beam on a copper target. A thermal shield was employed in this setup.

A weakness of the previous method is the lack of knowledge concerning the detailed overall pressure evolution, especially concerning variations of the setup. The effects of the addition/removal of a thermal shield must be studied to

establish comparability between measurements. This can be done by employing a gas dynamics simulation, which may also lead to a more sophisticated approach than using the ideal gas law.

GAS DYNAMICS SIMULATIONS

Molflow+ [5] is a Monte Carlo code that tracks gas particles in a given geometry. Its latest version is capable to simulate time dependant pressure evolutions in a given volume. Thus, it is well suited to gain further insights into the events after desorption and before/during the measurement. To illustrate this process, some selected moments of a simulated desorption process with a non pumping thermal shield are presented in Fig. 4. The beam travels from top to bottom, impacts on the target and desorption takes place (left panel). Here, the collimating influence of the shield's opening can be seen clearly. The desorbed gas plume spreads out into the available volume (center panel) and is either pumped by the turbomolecular pumps or reabsorbed onto the cold target.

An optional part of the experimental setup is the thermal shield. It is used to reduce the radiative heat load on the target to decrease T_{min} . During the U^{73+} beam time, the shield was not employed, so its effect on the pressure evolution must be understood in order to establish comparability between the measurements. To accomplish this, the employed measurement devices as well as the shield must be included into the simulation. Two extractor gauges are modeled by inserting a transparent tube of the size of the extractor's wirecage into the setup and by counting the particles passing through this volume. The impingement rates on this surface normalized to the number of desorbed particles is proportional to the pressure measured by the gauge. A plot of this value over time is presented in Fig. 5.

The extractor gauges used to measure the pressure evolution are read out with a sampling rate of 10 Hz, which is too low to resolve the desorption peak completely. To simulate this downsampling, measurement moments with a distance of 0.1 s are defined and time weighted averages of all values within an interval of ± 50 ms around the moment are calculated respectively. This spreads out the high, brief initial desorption peak over a tenth of a second.

The most obvious result is a difference in Δp by a factor of ca. 4 (for the gauge in the diagnostic chamber) to 8 (for the target chamber gauge) between the geometry with and without shield. Another effect of the shield is a slower pressure relaxation. This can be explained by a screening of the cold and gas adsorbing target by the non adsorbing shield. This lowers the vacuum conductance between the chamber, especially the volume near the target chamber gauge, and the cold target significantly.

In the simulation, the process described above takes place in a few tenths of a second, while it lasts up to several seconds in the measurements. A reason for this might be the instantaneous reflection of particles in the simulation code which neglects the sojourn time the particles spend adsorbed on the surface before being released again. Another reason

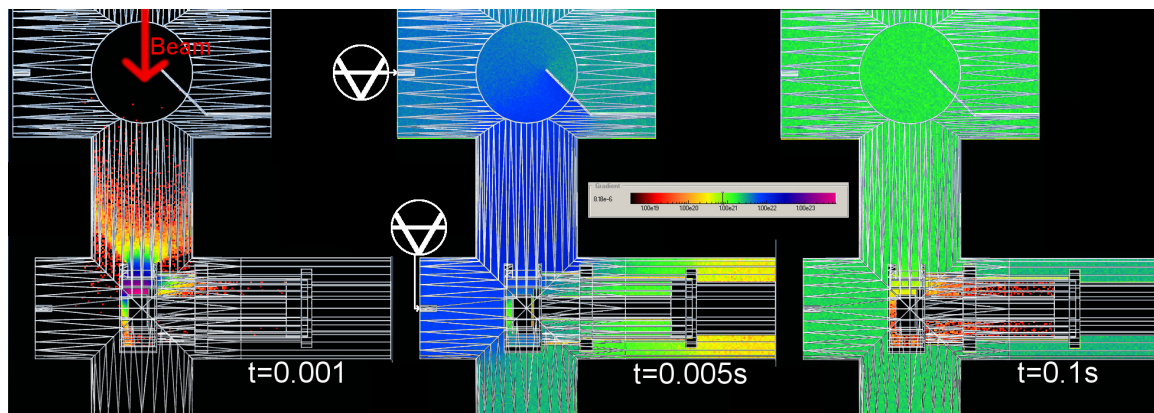


Figure 4: Three selected moments of a simulated desorption/pumping process with a non pumping thermal shield. The colour depicts the impingement rate of desorbed particles on a virtual plane through the center of the setup. $t = 0$ s is the moment of desorption. Two extractor gauges can be seen on the left sides of the pipecrosses. The top cross is called the diagnostic chamber, the lower cross is the target chamber. The former contains a model for a retracted scintillating target, which is used for beam positioning on the right flange, as well as a turbomolecular pump on the top flange.

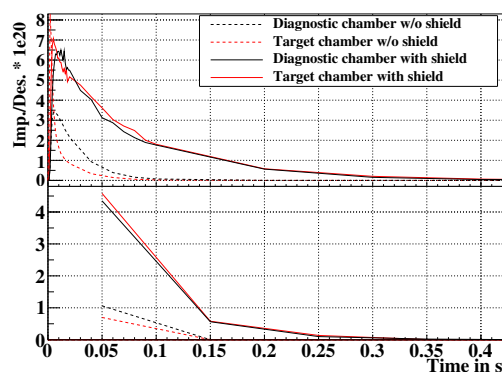


Figure 5: Plot of particle impingements per desorbed particle for both extractor gauges shown in Fig. 4, with and without a non pumping thermal shield. The upper panel shows a plot taken directly from the simulation while the lower panel takes the experiment's sampling rate into account.

might be the modeling of the extractor gauges. Therefore, a modification of the previous methodology has not been implemented yet.

Furthermore, the cold target constitutes a cryopump which decreases the height of the desorption peak. Evaluating the ratio between the particles pumped by the turbomolecular pumps and the particles adsorbed on the cold surfaces can lead to an estimate of the correction factor that needs to be introduced to account for such a readsorption process. In a warm, ideal environment, all desorbed particles are sooner or later removed by the turbomolecular pumps. But the cold target surface adsorbs 79.3% when being surrounded by the (non pumping) shield. In a simulation without a shield, this number rises to 90.4%. Therefore, the artificial decrease of the measured η , when cooling the target, is stronger for a setup with a thermal shield.

Although the time dependance of these ratios has not been examined yet, these numbers suggest that a lack of readsorption correction might be a responsible factor for the unexpected high cryogenic η presented in Fig. 3.

CONCLUSION AND OUTLOOK

Since the previous report [4], further heavy ion induced desorption experiments have been conducted in addition to a gas dynamic simulation. All room temperature measurements exhibit an η that scales with the electronic energy loss on the surface, but is much higher than in previous experiments. The reason for this is as of yet unknown. For the steel target, this scaling could also be seen in a cryogenic ($T_{\min} < 64K$) environment. In simulations, the thermal shield has been shown to have a significant effect on the measurements by screening the cold surface of the target. However the timescale on which the desorbed gas is pumped could not yet be reproduced, so no explicit correction factor could be found yet. Future work will seek to refine the simulation and correct for gas readsorption by the cold target.

REFERENCES

- [1] H. Kollmus et al., "Measurements of Ion-beam Loss Induced Desorption at GSI", AIP Conf. Proc. **773**, 207 (2005), p. 864
- [2] E. Mahner et al., Phys. Rev. ST Accel. Beams **14**, 050102 (2011)
- [3] L.H.J. Bozyk, H. Kollmus, P.J. Spiller, "Development of a Cryocatcher-System for SIS100", in Proc. of IPAC 2012, p. 3239
- [4] Ch. Maurer et al., "Heavy Ion Induced Desorption Measurements on Cryogenic Targets", in Proc. of IPAC 2014, p. 867
- [5] M. Ady, R. Kersevan, "Introduction to the Latest Version of the Test-particle Monte Carlo Code Molflow+", in Proc. of IPAC 2014, p. 2348